Promotion of surface energy closure by monitoring tree biomass heat storage

Biomass heat storage is important for promoting energy closure in forest ecosystems; however, this issue is often ignored in surface energy budgets. To determine an accurate approach to calculate biomass heat storage, we monitored the stem temperature of *Pinus sylvestris* in different heights, depths and orientations. At the same time, air sensible and latent heat storage and soil heat storage are also monitored together with biomass heat storage to study the heat storage share in surface energy budgets. The results showed that (1) temperature in different heights, depths and orientations in stem showed obviously differences dynamics, and time lags are existed between different measuring points inside stem. (2) Tree biomass heat flux varied around 12 W m^{-2}. Soil heat flux and air heat storage were around 20 W m^{-2} and 8 W m^{-2} separately, but out of phase with biomass heat flux. (3) Total heat storage in soil, biomass, and air was 60 W m^{-2}, accounting for ~10% of net radiation, which is a significant proportion of the total energy flux. This study will help improve biomass heat storage models and contribute to fundamental knowledge regarding energy balance closure in forest ecosystems.

PeerJ Preprints | https://doi.org/10.7287/peerj.preprints.2328v1 | CC BY 4.0 Open Access | rec: 1 Aug 2016, publ: 1 Aug 2016

Promotion of surface energy closure by monitoring tree biomass heat storage

Ming-Han Yu [1,2,3], Guo-Dong Ding [1,2,3*], Guang-Lei Gao [1,2,3], Yuan-Yuan Zhao [1,2,3], Ke Sai [1,2], Xu Li [1,2], Yue Wang [1,2] ,Yun-Dong Liu [1,2]

[1] Yanchi Research Station, School of Soil and Water Conservation, Beijing Forestry University, Beijing, China

[2] Key Laboratory of State Forestry Administration on Soil and Water Conservation, Beijing Forestry University, Beijing, China

[3] Engineering Research Center of Forestry Ecological Engineering, Ministry of Education, Beijing Forestry University, Beijing, China

Corresponding Author:
Guo-Dong Ding
35 East Qinghua Road, Haidian District, Beijing, 100083, China
Email address: dingguodong@bjfu.edu.cn (G.-D. D.)

PeerJ Preprints | https://doi.org/10.7287/peerj.preprints.2328v1 | CC BY 4.0 Open Access | rec: 1 Aug 2016, publ: 1 Aug 2016

Abstract: Biomass heat storage is important for promoting energy closure in forest ecosystems; however, this issue is often ignored in surface energy budgets. To determine an accurate approach to calculate biomass heat storage, we monitored the stem temperature of *Pinus sylvestris* in different heights, depths and orientations. At the same time, air sensible and latent heat storage and soil heat storage are also monitored together with biomass heat storage to study the heat storage share in surface energy budgets. The results showed that (1) temperature in different heights, depths and orientations in stem showed obviously differences dynamics, and time lags are existed between different measuring points inside stem. (2) Tree biomass heat flux varied around 12 W m^{-2}. Soil heat flux and air heat storage were around 20 W m^{-2} and 8 W m^{-2} separately, but out of phase with biomass heat flux. (3) Total heat storage in soil, biomass, and air was 60 W m^{-2}, accounting for ~10% of net radiation, which is a significant proportion of the total energy flux. This study will help improve biomass heat storage models and contribute to fundamental knowledge regarding energy balance closure in forest ecosystems.

Keywords: Plant temperature; biomass; heat storage; energy closure; near-surface

PACS: 87.23.-n

1. Introduction

Monitoring energy exchanges between the soil, the vegetation and the atmosphere is important for meteorological, ecological and agronomical purposes. Over the last few decades, our understanding of energy exchange between the Earth's surface and its atmosphere has developed at an unprecedented rate. For example, more than 576 flux stations have been established worldwide (Ardo et al., 2008). At these sites, eddy correlation technology has been used widely for water, energy, and CO_2 flux measurements in different ecosystems (Aubinet et al., 1999). However, flux observations have generally been inaccurate with respect to energy balance closure (McCaughey & Saxton, 1998; Dolman et al., 2002; Barr et al., 2006; Ray & Wang., 2014). Theoretically, the difference between net radiation and soil heat flux should equate to sensible and latent heat fluxes. However, the observed sensible and latent heat fluxes are usually 10–30% less than the theoretical values (Lee, 1998; Twine et al., 2000; Sakai, Fitzjarrald & Moore, 2001; Culf, Foken & Gash, 2004; Leuning et al., 2012).

The reasons driving this imbalance are complicated. Foken (2006) found that the energy imbalance was correlated with low frequency aspects contributing to flux. In addition, Lee (2004) determined that turbulent flux observations were responsible for the lack of energy closure. Furthermore, there are uncertainties with respect to soil surface-layer heat flux and biomass heat storage. Biomass heat storage is normally absolutely low (Oncley et al., 2007). But in arborous forestry, the biomass heat storage will grows dramatically. For instance, Moore and Fisch (1986) found total heat storage fluctuations of ~80 W m^{-2} in a tropical forest with high biomass content per unit of ground area. So, heat flux in biomass is non-negligible when studying energy exchange in forest areas. In fact, biomass heat storage is becoming increasingly significant in forest ecosystems.

To model energy balance, temperature dynamics should be evaluated. Temperature in plant stem, leaf, or root represents the balance between input and loss of energy (Yu et al., 2015). For a plant, leaf temperature can be significantly influenced by air temperature, which may be ignored due to its low biomass capacity (Burrage, 1972; Yu et al., 2015). Roots are under the ground and hard to be measure, so it is usually ignored in studies. Then, stem temperature is extremely important in determining plant energy balance. In addition, soil and air temperature are necessary in valuing heat storage in soil and near-surface air.

Therefore, the objectives of this study were to (1) measure the temperature in plant stems and explore their dynamics; (2) characterize heat storage in biomasses, soil and air; and (3) promote accurate near-surface energy balances.

2. Materials and Methods

2.1. Study area

The study was conducted in Yulin, Shaanxi Province, China (36°57′–39°35′N, 107°28′–111°15′E, 1,100 masl). This area is characterized by a mid-temperate semiarid continental monsoon climate. The average air temperature ranges from -7.8–37.5 ℃. The annual precipitation and evaporation are 397 and 2,491 mm, respectively. The annual sunlight ratio is 2,593.5–2,914.4 h. The soil is deep, lean aeolian soil. Large temperature differences between day and night and long hours of daylight lead to intense heat exchanges.

From April to September in 2015, the field investigation was conducted in a *Pinus sylvestris* var. *mongolica* Litv plantation, which is a common forest in the study area. All the trees are planted on an approximately flat ground and the whole forest casted about 300 hm^2. The basic conditions of the plantation are listed in Table 1.

Table 1. General information of the *P. sylvestris* plantation.

Stand age (a)	Mean diameter at breast height (cm)	Mean height (m)	Mean crown (m)	Canopy coverage (%)	Stand density (N ha^{-1})
30	20.1	10.6	6.3	70	1420

2.2. Field monitoring

2.2.1. Meteorological measurements

Microclimate data were collected automatically every 10 s and stored every 30 min with equipment fixed at a height of 10 m above ground level on a flux tower. The data were collected and processed in real time to provide near-continuous measurements. Air temperature and relative humidity (RH) were measured with a thermometer/hygrometer (HMP155A; Vaisala, Vantaa, Finland). Wind velocity (V) was determined using a Solent 3D Ultrasonic Anemometer (R2 Gill Instruments, Lymington, UK). Solar radiation (R) was measured using a four-component radiometer (CNR 4; Kipp & Zonen, Delft, The Netherlands). Air temperature and RH in the canopy were measured with thermocouple thermometers (L-95, Hai-Xu, China), mounted at 0, 2, 4, 6, and 10 m on branches of the target tree.

2.2.2. Soil heat flux

Soil heat flux was measured directly by three four-thermocouple heat flux plates (HFT-1; REBS, Seattle, WA, USA) installed 0, 5, and 10 cm below the soil surface. The voltage signals from the sensors were measured and stored with data loggers (CR10; Campbell Scientific, Inc., Logan, UT, USA) at 30-min storage intervals.

2.2.3. Biomass temperature

We used a typical or "standard" tree (whose size meet the mean value of the trees in the study area) to obtain the average value of the sample plot. Its diameter at breast height was 21.9 cm, height was 10.6m and crown was 5.7×6.2m. The standard was selected with no other trees too close to it, so it can get rid of being influenced. Biomass temperature was measured using thermocouple thermometers (0233, Ya Xin, China) with sensors inserted into the stem 0, 2, 4, 6 cm from the base of the stem. The last 10 mm of the sensors consisted of copper/constantan thermocouples with 0.1-mm diameters. Each sensor was inserted into the biomass at different depths through an aluminum tube fixed into a 3-mm diameter drilled hole. Resin formed by the tree quickly sealed the gap between the aluminum tube and the tree body. The connections between the sensors and data collector were held firmly in place by taping them around the stems. The tape is no reflective.

Temperature measurements in the standard tree were obtained for the analysis. Temperatures were measured at different heights, azimuthal positions, and depths in the stem as shown in Table 2.

Table 2. Positions of stem temperature sensors.

Height (m)	Stem diameter (m)	Bark thickness (m)	Depth (m)	Sensor azimuths (m)
0	0.252	0.020	0.03,0.05,0.08,0.10	N, S
2	0.198	0.017	0.03,0.05,0.08,0.10	N, S
4	0.172	0.011	0.03,0.05,0.08,0.10	N, S
6	0.156	0.006	0.03,0.05,0.08,0.10	N, S
breast height	0.219	0.017	0.03,0.05,0.08,0.10	N, S, E, W

2.3. Data analysis

2.3.1. Biomass heat storage

Energy transfer in plant stems is an important factor for regulating temperature dynamics in plant stems. The energy flux into physical storage is defined by the product of the rate of temperature change ($\Delta T/\Delta t$) and the heat capacity of the system (C_p m, where m is the mass in kg) (Haverd et al., 2007). We represented the heat storage rate in stems (S, in J s^{-1} or W) as follows:

$$S = (\Delta T / \Delta t) \cdot C_P m \quad (1)$$

The specific heat capacity, C_p (J $kg^{-1}K^{-1}$), indicates the amount of energy required to raise the temperature of unit mass by 1 ℃. We used a value of C_p (2,800 J kg^{-1} K^{-1}) for the stem in *P. sylvestris* (Jones, 1983). m is the biomass that undergoes a change in temperature ΔT according

to the time interval Δt, which we estimated as 450 kg m^{-3}. In practice, when studying the energy balance of vegetation canopies, the heat capacity of the leaves is frequently ignored, because energy storage in leaves is limited due to their small biomass.

The basic data on biomass quantity and physical characteristics are listed in Table 3. First, we determined the approximate fractions of different tree compartments based on similar densities. We used a drilling tool to obtain specific volumes of wood, at all of the heights at which temperature was measured, and weighted the volumes. We then averaged the weights and calculated the mean fresh stem density. The average amount of biomass in the sample plot was 13.039 kg m^{-2} (Table 3). The heat storage per area was estimated based on the number of *P. sylvestris* trees.

Table 3. Volume and fresh weight for the different stem segments

Height interval (m)	Radius up/ down (m)	Volume (m^3)	Fresh density (kg m^{-3})	Mass per tree (kg)	Number of trees per hectare (N ha^{-1})	average amount of biomass (kg m^{-2})
0-2	0.198/0.252	0.081		36.227		5.144
2-4	0.172/0.198	0.057		25.588		3.634
4-6	0.156/0.172	0.043	450	19.403	1420	2.755
6-10.6	0/0.156	0.024		10.603		1.506
total		0.204		91.821		13.039

Because biomass temperature varies at different heights, azimuthal positions, and depths, so to model biomass energy balance, we need to divide the biomass into isothermal subvolumes, which are generally referred to as nodes in heat transfer studies. As is shown in Figure 1, the stem is divided into various layers vertically (a), and the stem is divided into surface nodes and many interior nodes in one layer section (b). The interior nodes conduct heat to or from surface nodes as well as to or from other interior nodes. No matter surface or interior nodes, when they are very small, each node has a uniform temperature (Lewis & Nobel, 1977).

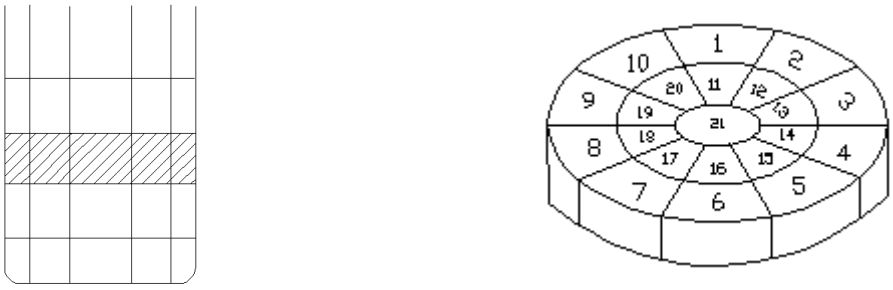

(a) (b)

Figure 1. Example of nodes or subvolumes used in biomass heat storage studies in forest stem. (a) vertical section indicating the division of the stem into various levels; (b) one of the horizontal section indicating the surface and interior nodes (1 to 21). Ideally, the stem should contain unlimited number of nodes or subvolumes.

Then, the heat storage rate equation in stems [Eq.1] can be adapted into:

$$S = \sum_{i=1}^{n} (\Delta T_i / \Delta t) \cdot C_{P_i} m_i \tag{2}$$

We approximately take C_p and m_i as uniform in different nodes. Then the equation can be simplified with just one variable $\Delta T_i/\Delta t$. It is expressed as follows:

$$\begin{aligned} S &= \sum_{i=1}^{n} (\Delta T_i / \Delta t) \cdot C_P m \\ &= (\Delta T_1 / \Delta t + \Delta T_2 / \Delta t + \cdots \Delta T_n / \Delta t) \cdot C_P m \\ &= (\Delta T_1 + \Delta T_2 + \cdots \Delta T_n) \cdot C_P m / \Delta t \\ &= [(T_1 - T_{1-\Delta t} + T_2 - T_{2-\Delta t} + \cdots T_n - T_{n-\Delta t})] \cdot C_P m / \Delta t \\ &= [(T_1 + T_2 + \cdots T_n) - (T_{1-\Delta t} + T_{2-\Delta t} + \cdots T_{n-\Delta t})] \cdot C_P m / \Delta t \\ &= (\mathrm{n}\, T_{mean} - \mathrm{n}\, T_{mean-\Delta t}) \cdot C_P m / \Delta t \\ &= \Delta T_{mean} / \Delta t \cdot C_P m \cdot \mathrm{n} \\ &= \Delta T_{mean} / \Delta t \cdot C_P \cdot M \end{aligned} \tag{3}$$

M is the total mass of the sectional stem. $\Delta T_{mean-\Delta t}$ is the mean temperature of the whole cross-section in a time space before. ΔT_{mean} has to be calculated so as to obtain the S value. Obviously, ΔT_{mean} can be expressed as T_{mean} - $T_{mean-\Delta t}$. To get T_{mean}, Kriging interpolation was used to model the data of the whole cross-section. Then, we averaged all of the data to obtain the T_{mean} of per cross-sectional area. Similarly, we can get $T_{mean-\Delta t}$ with the data of the whole cross-section in a time space before. With T_{mean} and $T_{mean-\Delta t}$ we got ΔT_{mean}, and we finally calculated the heat storage value S of each cross-section layer. After summing the S of all cross-section layers, we got heat storage value S of the whole tree.

2.3.2. Soil heat storage

Soil has a relatively high heat capacity. To raise the temperature of 1 kg of dry sand by 1 ℃ requires ~0.82 kJ. The density of soil solids is about 2,600 kg m^{-3} and, as soil is partly pores by volume, the density of dry soil is 1,500 kg m^{-3} (measured by drying undisturbed soil). Therefore, the volumetric heat capacity at constant pressure, C_p, of dry soil is about 0.82 kJ kg^{-1} $℃^{-1}$. As the average soil moisture in our experimental area was 8.8%, the water had a C_p of 4.18 MJ m^{-3} $℃^{-1}$ such that the C_p of soil was 1.57 MJ m^{-3} $℃^{-1}$, we defined it as C_v. The relatively high heat capacity of soil means that considerable energy can be involved in changes in its temperature.

Using equation (4), we calculated the heat storage of soil in the surface layer (0–10 cm):

$$G = G_z + \int_0^z c_v \frac{\partial T_s}{\partial t} dz \tag{4}$$

where G is the heat storage in soil, G_r is the soil heat flux 10 cm below the soil surface, T_s is the soil temperature in each layer from z below the ground to the surface layer, t is time, and C_v is the volumetric heat capacity.

2.3.3. Air heat storage

Air heat storage was divided into two parts: sensible heat and latent heat in air. For the storage calculations, air temperature and humidity at five heights (0, 2, 4, 6, and 10 m) were used. We calculated heat and humidity content in a column between 0–10.6 m by adding the contents in columns 0–2, 2–4, 4–6, and 6–10.6 m, where the average temperature in the first column (0–2) was equal to the mean of temperatures at 0 and 2 m, and 2–4 m was equal to the mean of temperatures at 2 and 4 m, etc. A similar method was followed for calculating water vapor content. These calculations were based on the 30-min mean data.

Storage of sensible heat in the air is theoretically calculated using the following equation:

$$S_{sensible} = \rho c_p \int_0^{z_{plate}} \frac{\partial T}{\partial t} dz \tag{5}$$

Storage of latent heat due to phase shifts in air water column is given by:

$$S_{sensible} = \rho L \int_0^{z_{plate}} \frac{\partial q}{\partial t} dz \tag{6}$$

where q is the specific humidity of air.

3. Results

3.1. Biomass temperature

3.1.1. Decreased temperature in the stem

The temperature in the stem decreases rapidly from the bark surface inwards (Fig. 2). The largest gradient is close to the stem surface in the daytime. The gradient in maximum temperature between 30 and 50 mm depths is around 3 ℃ during a sunny day. The gradient in maximum temperature between the 80 and the 100 mm depths is much smaller, only in the order of 1 ℃. We hypothesized that the heat capacity of the stem caused the differences between deep and surface measuring points.

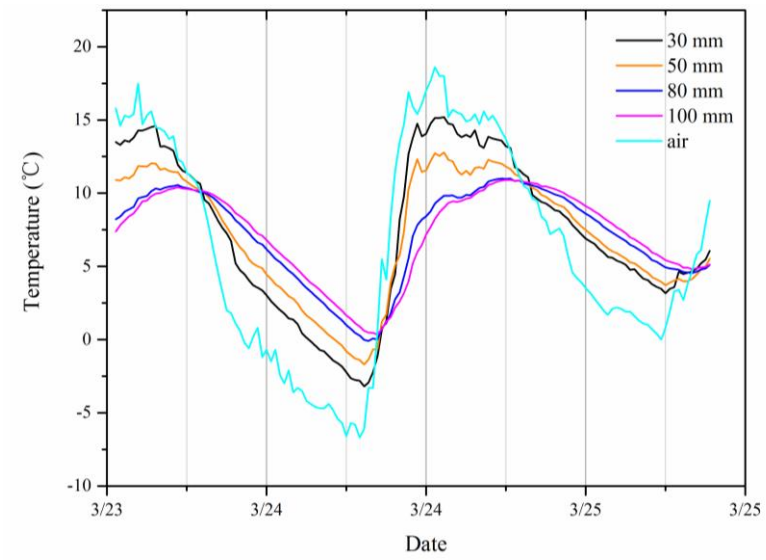

Figure 2. The temperatures at different depths from the bark surface and inwards in the trunk of the target tree at breast height above ground.

The phase shift is also obvious; the 30 mm sensor value reaching its maximum 10–20 min after high noon (12:00), whereas the 100 mm sensor value reaches its maximum about 5 h later. It can also be seen that at 30 mm, the temperature shows a much wider small-scale variation than temperatures at larger depths in the stem. We hypothesize that these small-scale variations are caused by the thermal properties of the stem, which results in that shallow one is more sensitive to surroundings.

3.1.2. Temperature differences at different orientations

The temperature changes at different orientations, decreasing rapidly from the sunny to the shaded side (Fig.3). At high noon, temperature has a large gradient from the south to the northwest direction, commensurate with changes in the direction of the sun in the afternoon. The phase shift is also obvious with values at the S30 and E30 sensors reaching their maximum 10–20 min after noon, while the values at the N30 and W30 sensors reach their maximum about 5 h later. It can also be seen that the values at the S30 and E30 sensors show a much wider small-scale variation than those at the N30 and W30 sensors in the stem.

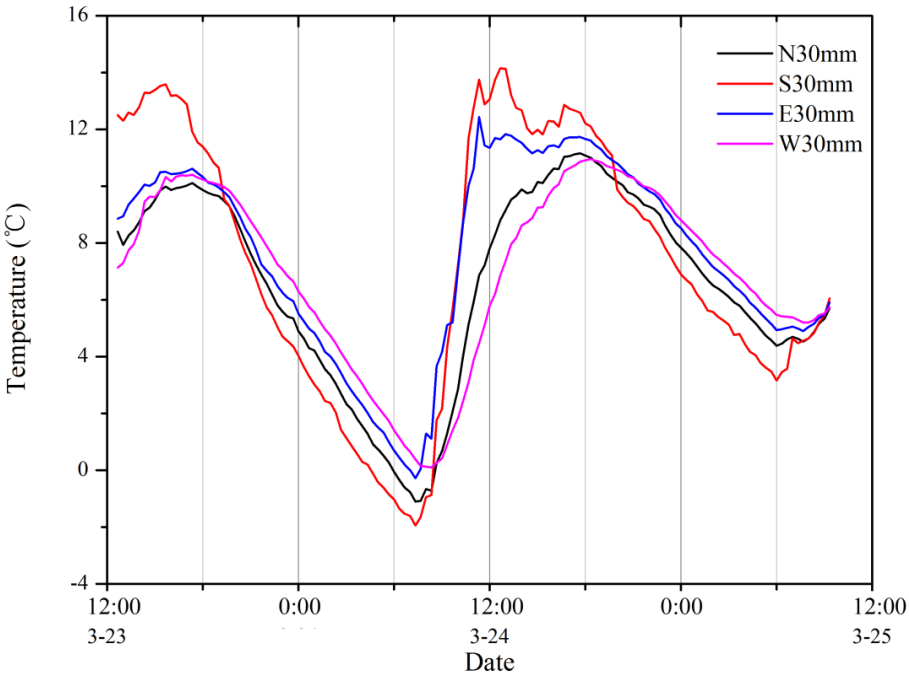

Figure 3. The azimuthally trunk temperature (30mm in depth) at different orientation around the trunk at breast height above ground. The N, S, E, W are short for orientations of north, south, east and west separately.

3.1.3. Vertical gradient in temperature

There is also a significant vertical gradient in temperature along the stem, with maximum temperatures increasing commensurate with increasing height along the stem (Fig. 4). The temperature difference between the base of the tree (0 m) and the highest point in the canopy (6 m) is ca. 10 ℃. At night, however, the temperature difference at different heights is much smaller, ca. 4 ℃, and in the reverse order (such that the highest level is also the coolest, with the lower levels becoming warmer except for at 0 m, at which the temperature was significantly

influenced by surface soil temperature). Temperature in the southerly direction (Fig. 4 S) in lower layers shows much smaller amplitudes than upper layer temperatures. In addition, gradient is particularly obvious at high noon when temperatures cool by 6 to 8 ℃ from 0 to 2 m, whereas from 4 to 6 m there are only ca. 2 ℃ differences. Temperature in the northerly direction (Fig. 4 N) shows a similar tendency to that in the southerly direction.

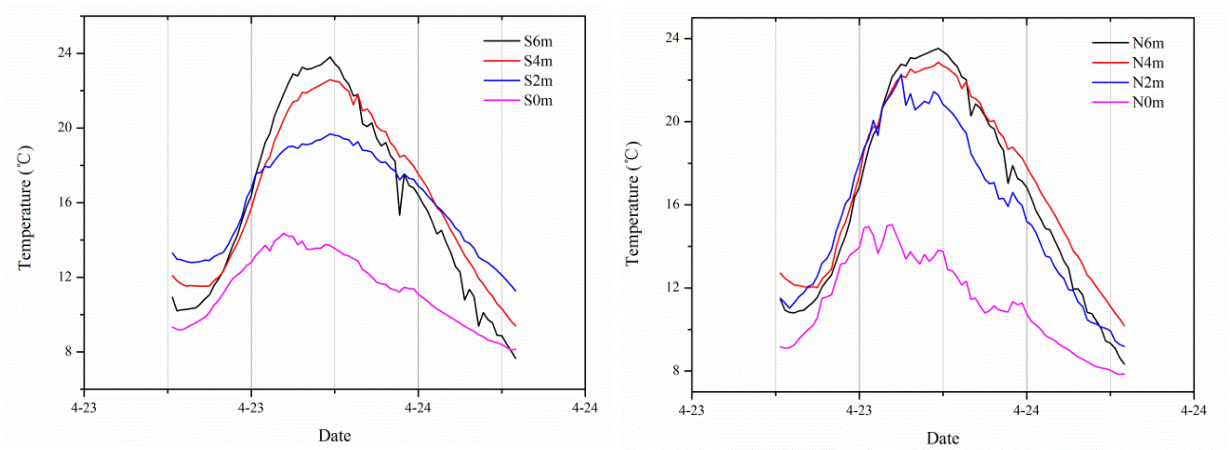

(a) (b)

Figure. 4 The trunk surface temperature (30 mm in depth) at different heights along the trunk of a *P. sylvestris* tree as well as the temperature of the air. A is the temperature in south direction, while B is the temperature in north direction.

3.1.4. Mean temperature of the crossing section

Kriging interpolation showed the whole temperature distribution of the crossing section (Fig. 5A). The center of the temperature distribution (i.e., the most stable value) is somewhat close to the northeast side. We supposed that this unsymmetrical phenomenon was the result of solar irradiation (energy source) coming from a southwestern direction and rendering the stem temperature more sensitive than in the northeastern direction.

The contour lines in the temperature distribution of the crossing section showed great differences within a single day. The temperature is significantly different between the central part and edge of the stem. From 20:00 to 08:00 the next day, the temperature in the central stem is warmer than at the edge. Heat is transferred from the inside to the outside. From 10:00 to 18:00, the temperature inside the stem is cooler than that outside the stem, such that heat is transferred in the opposite direction.

Daily T_{mean} calculated using Kriging interpolation showed diurnal variation (Fig. 5B), with an amplitude that was relatively smoother than for that air temperature. The highest peak T_{mean} appeared at around 18:00, which was 5 hours later than for the air temperature; meanwhile, the lowest peak value appeared at around 09:00, about 1 hour later than the air temperature.

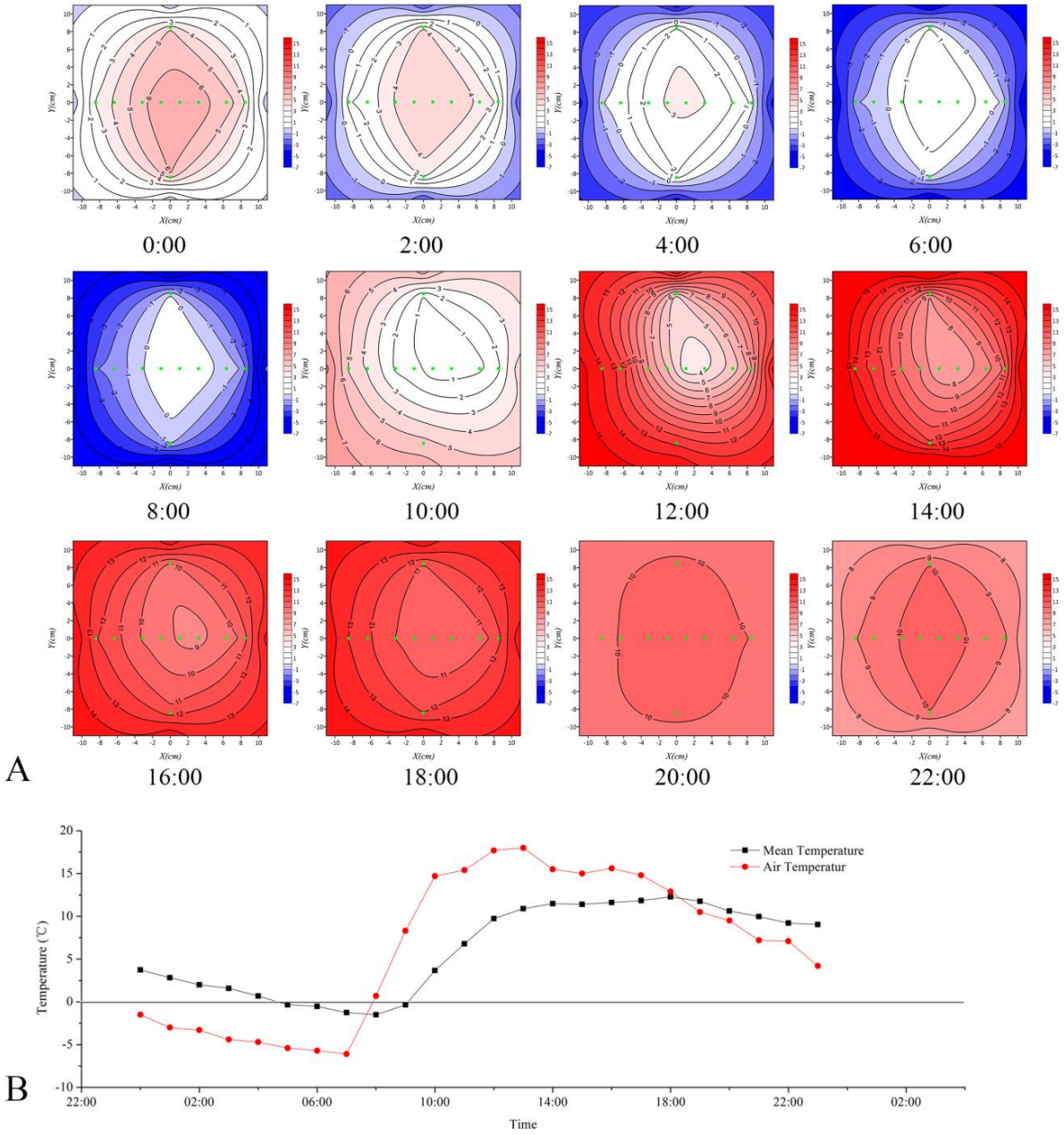

Figure 5. The temperature distribution of the cross-section at breast height and daily variances by every two hours. A:The temperature distribution is based on the result of Kriging interpolation. B: Daily dynamics of the mean temperature with comparative to the air temperature by hours.

For time-consuming and inconvenient of multi-point measurement, so we furthered to try to find a representative measuring point for instead of measuring the T_{mean}. We used a correlation analysis between the T_{mean} and all measured values to determine a representative point that maximized the relevance of the model. Then, using the relationship model between T_{mean} and the representative point data, we evaluated T_{mean}.

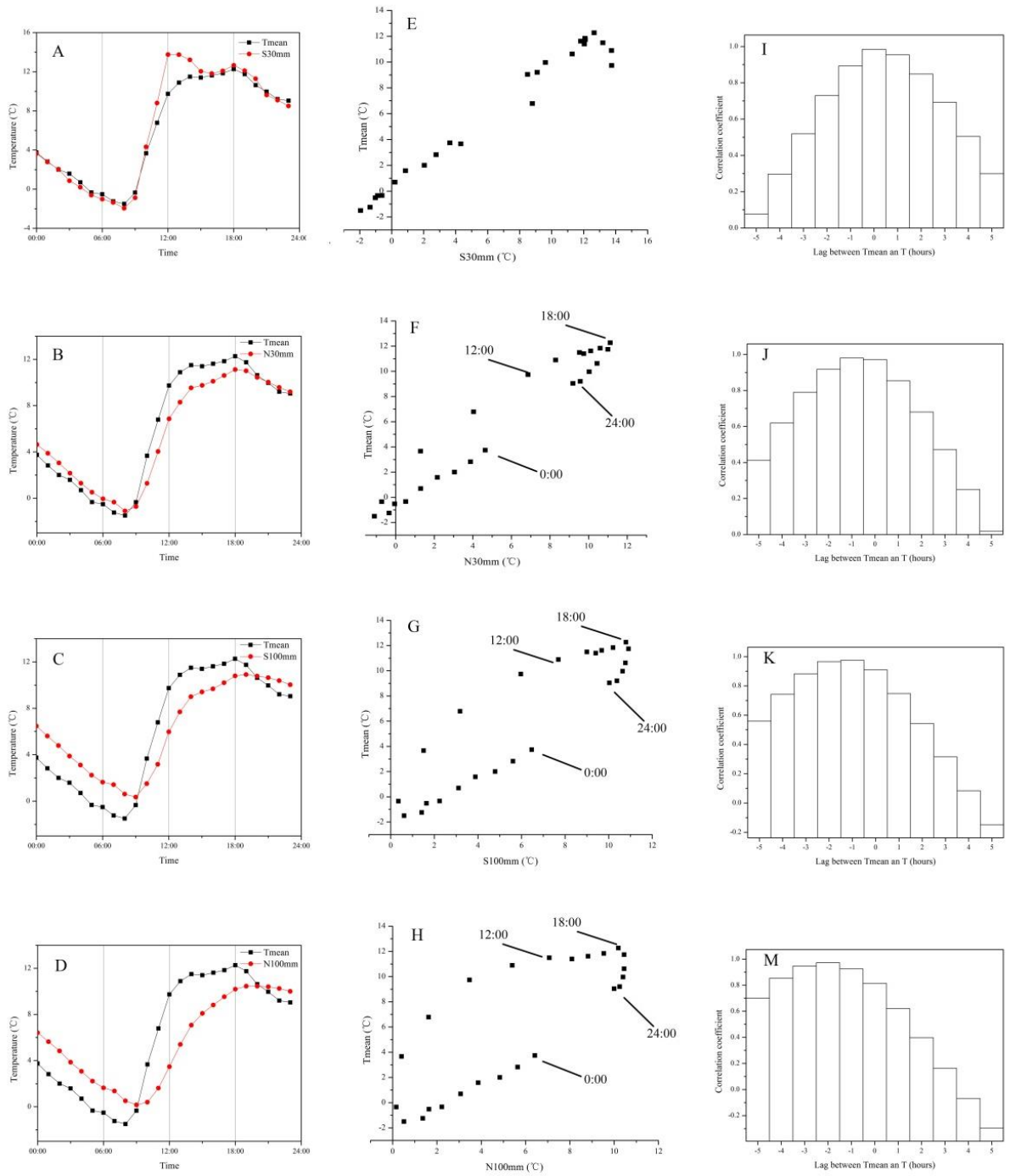

Figure 6. Diel cross-section mean temperature (T_{mean}) and temperature in the measuring points S or N (A–D), diel T_{mean} vs. measuring points S or N (E–H), their lag correlations (I–M). Mean values for July are shown. Black circles in (A–D): T_{mean} ; Red circles in (A–D): S or N. The dashed lines in (I–M) are reference lines for the zero lag.

From figure 5 we got that the lag between diel oscillations in T_{mean} and temperature at the measuring points showed a strong azimuthal and deep pattern, with almost no lag at S30 mm (the 30-mm deep measurement point in the south) but lags of up to 2 hours at N100 mm (the

100-mm deep measurement point in the north) (Fig. 6A–D). The lag between temperature in the northerly direction and at the deep position led to hysteresis loops (Fig. 6F–H), and the correlation between T_{mean} and N100 mm was strongest after lagging T_{mean} by 2 hours (Fig. 6M). In contrast, T_{mean} was in phase at S30 mm (Fig. 6E), with the zero lag value generating the highest correlation coefficient (Fig. 6I). We chose S30 mm as the parameter with which to model T_{mean} with the equation $y = 0.8743x + 0.4241$($R^2 = 0.9688$). With the calculated T_{mean}, we may evaluate heat storage flux in the stem when we have no sufficient measurement devices.

3.2. Biomass heat storage

3.2.1. Diel temperature response of S

It was assumed that the four stem temperature measurement levels, 0, 2, 4 and 6 m, represented stem sections at 0–2, 2–4, 4–6 and 6–10.6 m, respectively, to calculate heat storage at each level (Fig. 7). Although the segment in the upper layer had the highest heat flux value (Fig. 4), biomass in this segment was also relatively lower than that of the rest of the tree (ca. 8%) (Table 3), so it does not capture the largest proportion of heat. Similarly, the segment in the bottom layer holds the largest amount of biomass (ca. 40%) but has an excessively low heat flux value, resulting in a low proportion of stored heat. Thus, the stem segment at 2–4 m contributed most to the stem heat storage of trees, because it was associated with both a relatively large biomass and high flux. The biomass data is presented in Table 3, and the heat flux values are shown in Fig. 4.

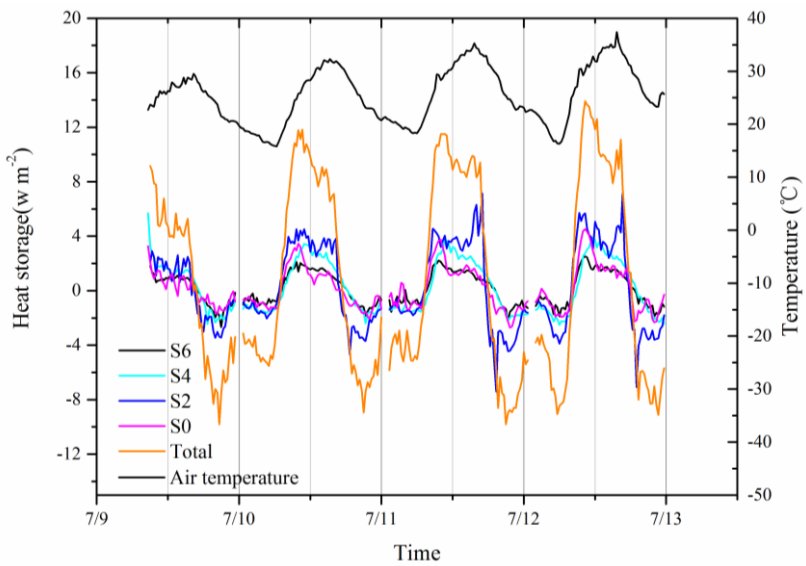

Figure 7. The estimated biomass heat storage flux from different height intervals during the four days in July.

3.2.2. Seasonal pattern of S

Daily total heat storage in the target tree is shown in Fig. 8, which demonstrates both positive and negative values. Amplitude of variation was lowest in April, but remained high throughout the summer before decreasing after mid-August. Daily total heat storage in April

ranges from -40 to 40w m^{-2}, while in other months the storage ranges from -80 to 80 w m^{-2}; there was strong seasonality over the year. The mean value of daily total heat storage in 1 month is around zero, which means that the incoming and released energy is in balance, with no seasonal differences.

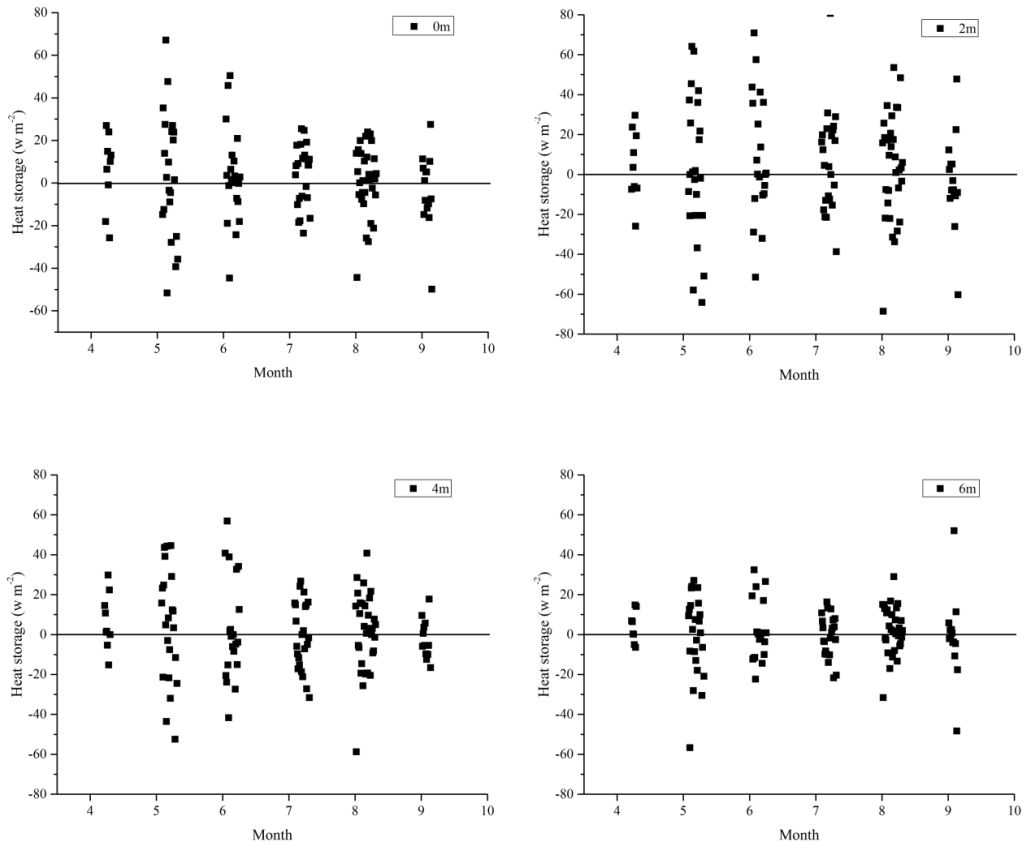

Figure 8. The estimated daily biomass heat storage from different height intervals during the growing season in 2015.

3.3. Soil heat storage

During the up-scaling procedure, it was assumed that the three soil temperature measurement levels, 0, 5 and 10 cm underneath the soil surface, represented stem sections at 0–2, 2–6, and 6–10 cm, respectively. We measured, somewhat arbitrarily but also reasonably, the layered soil in centimeters and assumed that the temperature gradient was reduced to a greater extent in the upper soil layer. In fact, the degree of heat storage in the soil differed greatly in the vertical direction. The soil surface can exhibit large daily oscillations in heat flux, ranging around 40 W m^{-2} in the upper 2 cm layer around noon (Fig. 9), while soil heat flux at moderate depths (e.g., of 10 cm) can remain very steady throughout a single day (i.e., variations of less than 5 W m^{-2}). The upper layer segment has the highest heat storage value, even though it also holds a relatively lower proportion of the whole soil volume (ca. 20%), because of the large heat flux. The segments at the two deeper layers hold the same volume of soil (ca. 40%), but the section at 6–10 cm has the low heat flux value, resulting in a low proportion of heat storage. Thus, the upper layer segment (0–2 cm) contributed most to the soil heat storage, because it is readily influenced by the ambient environment. Time lag is significant between the different

soil layers. When the upper layer (0–2 cm) reached its highest heat storage value, the values at 2–6 cm and 6–10 cm remained under zero. The large time lag resulted in a smoother phase shift with respect to total heat storage.

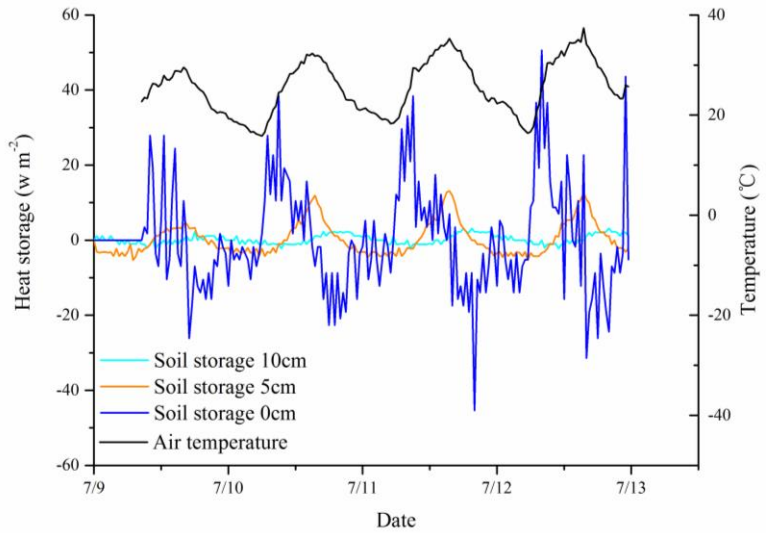

Figure 9. The estimated soil heat storage from separated layers during the four days in July.

3.4. Total and proportional energy balance

When all of the storage components are taken into account (soil, air and biomass), the total storage flux in the layer near the surface ranges between +60 and −60 W m^{-2} during the four-day period in July shown in Fig. 10. The maximum biomass storage flux is about half of the maximum flux in the soil. The biomass heat storage in the stem varies between +12 and −12 W m^{-2}, while the surface soil heat storage varies between -20 to 20 W m^{-2}. The air heat storage varies between -8 to 8 W m^{-2}. The soil storage flux peaks 3–4 h before the biomass peak. The air storage flux peaks 1–2 h before the biomass peak. Because of the different time lags among the different storage components, the curve representing the total storage flux is slightly skewed towards the earlier part of the day (Fig. 10).

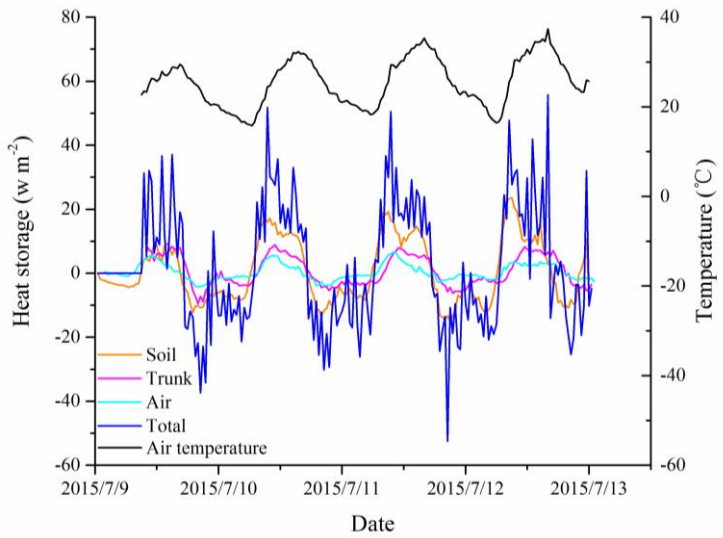

Figure 10. The storage flux of the entire stand divided into stem, soil and air during four summer days.

4. Discussion

4.1. Temperature dynamics in the stem

The direction, depth and height of the detection points significantly influence the measured temperature. The relationship between the value at a single point and the air temperature showed obvious time lag (Fig. 6).

Deeper measurement points have longer time lags than surface points, and measuring point value in a northerly position is much more likely to achieve hysteresis effects. Time constants can be used to explain the results. We defined time constant as being related to heat storage, with respect to temperature changes in response to changes in environmental conditions. Usually, time constant refers to the time required for a change in the surface temperature, from some initial value to within a certain volume of the overall change to a final value. Time constant is related to the mean depth of heat storage in a given surface area, and also to the volumetric heat capacity we referred to previously. Indeed, massive stems show large time constants for thermal changes, which means that temperature changes in the stem are much slower compared to changes in the ambient environment; this accounts for the time lag.

So we cannot use one data point to represent the whole tree, but a roughly representative point can be obtained with which to model average temperature in a given tree section. From our measured results, time lag appears to barely exist at the surface measuring point (30 mm) in the southerly direction, which is in the same phase as T_{mean}; therefore, we used the value at this point to model the T_{mean}.

4.2. Dynamics of heat storage in biomass

Estimation of biomass heat storage is very complicated because of the varying temperature in tree stems and requires a large number of sensors (Nobel, 1975; Oliphant *et al.*, 2004; Roupsard *et al.*, 2006). Normally, for more accurate modeling, stem temperature dynamics should be detected using multiple sensors, due to variance among different measuring points, usually followed by division into isothermal subvolumes. By calculating heat storage rates in each subvolume, the total value can be obtained by summing the subvolumes (Nobel, 1991). The high workload and requirement for intense sensors limits the efficiency of heat flux measurements and energy calculations. Therefore, a mathematical framework is needed for more convenient estimation of stem heat storage (Meesters & Vugts, 1996). In this study, we implemented cross-sectional multi-point measurements to evaluate the T_{mean} when calculating the heat capacity.

Heat storage in biomass shows daily and seasonal variations. The daily changes are mainly due to variations in air temperature. We showed that the heat storage response to air temperature is not due to the absolute value, but rather to the variance in values. Heat storage is high between 08:00–12:00, because the air temperature increases markedly at this time. However, after high noon, even though air temperature is still high, heat storage decreases because the ambient temperature is steady, with limited variance. Thus, we can explain why the phenomena of seasonal changes having no significant regulations. Seasonal changes in heat

storage are not significant, because the differences between day-and-night temperatures in each month are basically the same (Fig. 9). The day-and-night temperature difference in April and September is relatively low, such that heat storage values also showed a narrow fluctuation range.

However, the daily total heat storage in 1 month is basically around zero. This means that the incoming and released energy is balanced. We consider biomass to be a good buffer pool, with respect to the energy budget, for adjusting ecosystem balance.

4.3. The energy balance of heat storage

The maximum total heat storage, including biomass, air and soil, was ca. 60 W m^{-2} in one day in July in our study. Other studies in forests have reported values of up to 80–90 W m^{-2} (Michiles & Gielow, 2008), and in some cases, even up to 100 W m^{-2} (Tanaka *et al*., 2008). The main heat storage components are soil and biomass, which contribute approximately equally, although there are phase lags between these components.

One study showed that net radiation into the near surface of *P. sylvestris* forest in Yulin County (an area that is similar to the sample plot) reached up to 500 W m^{-2} in July (Chen, 2014). The heat storage we showed reached up to ca. 10% of the total net radiation, which makes up a large proportion of the energy closure. Tree biomass heat flux reached maximum values that were about 50% of the maximum values for soil heat storage, and contributed a large proportion of the energy closure.

It is interesting to note that so few studies have been concerned with heat storage components, particularly given the problems that exist with respect to closure of the energy balance. Much more work on heat storage needs to be carried on to resolve these issues. Storage in branches and leaves should be also concerned to realize more calculated accurately.

Of course, we present here only one case pertaining to the calculation of heat storage. In many cases, complex conditions require further consideration, such as under conditions of complicated terrain (i.e., an undulating surface), in which energy absorption and release is not uniform and one cannot simply take an average reading. Detailed information on the particular circumstances in an area must be obtained to make a concrete analysis.

Furthermore, heat storage does not linearly increase with plant density, because thicker forests limit the flow of energy in an ambient environment. The manner in which the plant characteristics relate to the energy balance in different storage components should be further studied by experiments in which density changes but other conditions are held constant.

5. Conclusions

The stem temperature is significantly influenced by direction, depth and height of the detection points and the relationship between the value at a single point and the air temperature showed obvious time lag. We implemented cross-sectional multi-point measurements to evaluate the T_{mean} when calculating the heat storage in this study. The result of tree biomass storage showed highly significant in the context of storage flux in a mature forest. Heat storage in soil, air and biomass captures almost 10% of the total energy income (net radiation). Good

energy closure can be attained by measuring fluctuations in heat storage. These findings have important implications for ecosystem energy balance modeling.

The English in this document has been checked by at least two professional editors, both native speakers of English. For a certificate, please see: http://www.textcheck.com/certificate/Qc57aZ

References

[1] Ardo, J.; Molder, M.; El-Tahir, B. A.; Elkhidir, H. A. Seasonal variation of carbon fluxes in a sparse savanna in semi-arid Sudan. Carbon Balance & Management 2008, 3, 1-18.

[2] Aubinet, M.; Grelle, A.; Ibrom, A.; Uuml; Rannik; Moncrieff, J.; Foken, T.; Kowalski, A. S.; Martin, P. H.; Berbigier, P.; Bernhofer, Ch. Estimates of the annual net carbon and water exchange of forests: the Euroflux methodology. Adv Ecol Res 1999, 30, 113-175.

[3] McCaughey, J.H.; Saxton, W.L. Energy balance storage terms in a mixed forest. Agr Forest Meteorol 1988, 44, 1-18.

[4] Dolman, H.; Field, C.; Grelle, A.; Ibrom, A. Energy balance closure at Fluxnet sites. Agr Forest Meteorol 2002, 113, 223-243.

[5] Barr, A.G.; Morgenstern, K.; Black, T.A.; McCaughey, J.H.; Nesic, Z. Surface energy balance closure by the eddy-covariance method above three boreal forest stands and implications for the measurement of the CO_2 flux. Agr Forest Meteorol 2006, 140, 322-337.

[6] Ray, G.A.; Wang, D. Energy budget closure observed in paired eddy covariance towers with increased and continuous daily turbulence, Agr Forest Meteorol 2014, 184, 204-209,

[7] Lee, X. On micrometeorological observations of surface-air exchange over tall vegetation. Agr Forest Meteorol 1998, 91, 39-49.

[8] Twine, T.E.; Kustas, W.P.; Norman, J.M.; Cook, D.R.; Houser, P.R.; Meyers, T. P.; Prueger, J. H.; Starks, P. J.; Wesely, M. L. Correcting eddy-covariance flux underestimates over a grassland. Agr Forest Meteorol 2000, 103, 279-300.

[9] Sakai, R.K.; Fitzjarrald, D.R.; Moore, K.E. Importance of low-frequency contributions to eddy fluxes observed over rough surfaces. J Appl Meteorol 2001, 40, 2178-2192.

[10] Culf, A.D.; Foken, T.; Gash, J.H.C. The energy balance closure problem. Springer: Berlin Heidelberg, Germany, 2004; pp. 159-166.

[11] Leuning, R.; Gorsel, E. V.; Massman, W. J.; Isaac, P.R. Reflections on the surface energy imbalance problem. Agr Forest Meteorol 2012, 156:65-74.

[12] Foken, T.; Wimmer, F.; Mauder, M.; Thomas, C.; Liebethal, C. Some aspects of the energy balance closure problem. Atmos Chem Phys 2006, 6, 4395-4402.

[13] Lee, X.; Massman, W.; Law, B. Handbook of micrometeorology : a guide for surface flux measurement and analysis. Kluwer Academic Publishers: Dordrecht, Holland, 2004, 23-34.

[14] Oncley, S.P.; Foken, T.; Vogt, R.; Kohsiek, W.; Debruin, H.A.R.; Bernhofer, C.; Christen, A.; Gorsel, E.; Grantz, D.; Feigenwinter, C.. The energy balance experiment EBEX-2000. Part I: overview and energy balance. Bound-Lay Meteorol 2007, 123, 1-28.

[15] Moore, C.J.; Fisch, G. Estimating heat storage in Amazonian tropical forest. Agr Forest Meteorol 1986, 38, 147-168.

[16] Yu, M. H.; Ding, G. D.; Gao, G. L.; Bao, Y. F.; Zhao, Y. Y.; Wan, L. How the plant temperature links to the air temperature in the desert plant *Artemisia ordosica*. Plos One 2015, 10, e0135452.

[17] Burrage, S.W. Atlas of energy budgets of plant leaves. Physiol Mol Plant P 1972, 2, 87-88.

[18] Yu, M. H.; Ding, G. D.; Gao, G. L.; Zhao, Y. Y.; Yan, L.; Sai, K. Using plant temperature to evaluate the response of stomatal conductance to soil moisture deficit. Forests 2015, 6, 3748-3862.

[19] Haverd, V.; Cuntz, M.; Leuning, R.; Keith, H. Air and biomass heat storage fluxes in a forest canopy: Calculation within a soil vegetation atmosphere transfer model. Agr Forest Meteorol 2007, 147, 125-139.

[20] Jones, H.G. Plants and microclimate: a quantitative approach to environmental plant physiology. Cambridge University Press: Cambridge, United Kingdom, 1983, 202-216.

[21] Lewis, D. A.; Nobel, P. S. Thermal energy exchange model and water loss of a barrel cactus, Ferocactus acanthodes. Plant Physiology 1977, 60:609-16.

[22] Nobel, P. S. Effective thickness and resistance of the air boundary layer adjacent to spherical plant parts. J Exp Bot 1975, 26:120-130.

[23] Oliphant, A.J.; Grimmond, C.S.B.; Zutter, H.N.; Schmid, H.P.; Su, H.B.; Scott, S.L.; Offerle, B.; Randolph, J. C.; Ehman, J. Heat storage and energy balance fluxes for a temperate deciduous forest. Agr Forest Meteorol 2004, 126, 185-201.

[24] Roupsard, O.; Bonnefond, J.M.; Irvine, M.; Berbigier, P.; Nouvellon, Y.; Dauzat, J.; Taga, S.; Hamel, O.; Jourdan, C.; Saint-André, L. Partitioning energy and evapo-transpiration above and below a tropical palm canopy. Agr Forest Meteorol 2006, 139, 252-268.

[25] Nobel, P.S. Physicochemical and Environmental Plant Physiology. Academic Press: America, 1991,34-52.

[26] Meesters, A.G.C.A.; Vugts, H.F. Calculation of heat storage in stems. Agr Forest Meteorol 1996, 78, 181-202.

[27] Michiles, A.A.D.S.; Gielow, R. Above-ground thermal energy storage rates, trunk heat fluxes and surface energy balance in a central Amazonian rainforest. Agr Forest Meteorol 2008, 148, 917-930.

[28] Tanaka, H.; Hiyama, T.; Kobayashi, N.; Yabuki, H.; Ishii, Y.; Desyatkin, R.V.; Maximov, T.C.; Ohta, T. Energy balance and its closure over a young larch forest in eastern Siberia. Agr Forest Meteorol 2008, 148, 1954-1967.

[29] Chen S.J. Research on eco-hydrological functions of secondary *Pinus tabulaeformis* forest in the Qinling Mountains. Doctor Thesis, Northwest A&F University. Yangling Shaanxi China, 2014.